Nuclear Physics B136 (1978) 77–94

A PARTIAL-WAVE ANALYSIS OF THE NEUTRAL 3π SYSTEM PRODUCED IN THE REACTION $\pi^- p \to (\pi^+\pi^-\pi^0)\, n$ AT 12 AND 15 GeV/c

M.J. CORDEN, J.D. DOWELL, J. GARVEY, M. JOBES, I.R. KENYON, J. MAWSON and T. McMAHON
University of Birmingham, UK

I.F. CORBETT, R.J. ESTERLING *, N.H. LIPMAN, P.J. LITCHFIELD and K.C.T.O. SUMOROK
Rutherford Laboratory, Didcot, Oxon, UK

G. ALEXANDER, S. DAGAN and Y. GNAT
Tel-Aviv University **, *Israel*

E.H. BELLAMY, M.G. GREEN, N. HARNEW, J.B. LISTER, J.R. LISTER, A.W. ROBERTSON ***, B.J. STACEY, J.A. STRONG and D.H. THOMAS +
Westfield College, London, UK

Received 19 December 1977

Data on the charge-exchange reaction $\pi^- p \to (\pi^+\pi^-\pi^0)\, n$ have been taken at beam momenta of 12 and 15 GeV/c, using the CERN Omega Multiparticle Spectrometer. A partial-wave analysis has been made of the $(3\pi)^0$ system. We observe both natural and unnatural spin-parity production. The natural parity states can be identified with established resonances. In addition a natural spin-parity enhancement is observed at a mass of about 2 GeV/c^2 with $J^P = 4^+$ preferred. We have called this effect the $A_2^*(2030)$. The unnatural spin-parity production found is consistent with reggeized Deck model predictions. No unambiguous A_1 or A_3 production is observed.

1. Introduction

The success enjoyed by the constituent quark model in predicting hadronic states is considerably clouded by the lack of experimental evidence for the axial

* Now at Philco-Ford, Philadelphia, USA.
** Supported by the Israel Academy of Science and Humanities, The Israel Commission for Basic Research.
*** Now at the Rutherford Laboratory, Didcot, Oxon., UK
\+ Now at CERN, Geneva, Switzerland.

vector mesons. To date the B(1235) $IJ^{PC} = 11^{+-}$ is the only positively identified $S = 0$ axial vector meson with the $|S| = 1, I = \frac{1}{2}$ states Q_A and Q_B as strong candidates [1]. Two possible $IJ^{PC} = 01^{++}$ candidates D(1285) and E(1420) await a definite spin-parity assignment. In the constituent quark model an $IJ^{PC} = 11^{++}$ state and two $IJ^{PC} = 01^{+-}$ states are also required, the former being known as the A_1. Analyses of the $(3\pi)^{\pm}$ system, produced in $\pi^{\pm}$p reactions, have shown a broad $IJ^{PC} = 11^{++}$ enhancement at about 1.1 GeV/c^2 with a slowly varying phase incompatible with a simple resonance interpretation. The reggeized Deck model provides a possible interpretation of this phenomenon [2]. The data, however, cannot rule out resonance production since this may be hidden under the diffractively produced $(3\pi)^{\pm}$ mass enhancement. New evidence has recently been reported for a resonant A_1 signal produced diffractively and also by baryon exchange [3].

In reactions where the $\pi^+\pi^-\pi^0$ system is produced *via* charge exchange no diffractive contribution is possible. Furthermore both $I = 0$ and $I = 1$ states are accessible in this three-pion system. Thus the $\pi^+\pi^-\pi^0$ system is better suited to the search for the "lost" axial vector mesons. Various experiments have now analysed the $\pi^+\pi^-\pi^0$ system produced in different charge-exchange reactions [4–6], but the elusive A_1 has not yet been observed in this system. Instead they find natural parity resonances together with a smoothly varying unnatural parity background.

In this paper we present the results of a partial-wave analysis of the three-pion system in the reaction

$$\pi^-\mathrm{p} \to \pi^+\pi^-\pi^0\mathrm{n}\,, \tag{1}$$

at 12 and 15 GeV/c using a modified version of the programme developed at the University of Illinois [7]. The data were obtained at the CERN Omega spectrometer using a slow neutron time-of-flight trigger. Descriptions of the Omega spectrometer facility, the experimental set-up and the neutron counter preformance are given in previous publications [8]. In sect. 2 the data are described. Further details concerning our data selection criteria and the acceptance of the apparatus are discussed in ref. [9]. The method of analysis is described in sect. 3 and the results presented in sect. 4. In sect. 5 we examine the quality of the fits by comparing the Monte Carlo predictions with various experimental distributions. Sect. 6 compares our results on the unnatural parity states with the predictions of a reggeized Deck model and sect. 7 contains our conclusions.

2. Description of the data

The event data were processed through the pattern recognition and geometrical reconstruction package ROMEO [10]. Following the geometrical reconstruction the data were processed with the Rutherford Laboratory Kinematics programme [11]. Events found ambiguous between channel (1) and the 4C channels $\pi^-\mathrm{p} \to \pi^+\pi^-\mathrm{n}$, $\mathrm{K}^+\mathrm{K}^-\mathrm{n}$ and $\bar{\mathrm{p}}\mathrm{pn}$ were removed from the sample. Events fitting other 1C

channels were selected on the basis of the highest χ^2 probability. A χ^2 probability cut of 5% was imposed.

Acceptance normalization integrals were calculated using Monte Carlo events tracked in a simulated Omega spectrometer [9]. Cuts were made inside the acceptance limits of the apparatus and real events lying outside the cuts were removed from the sample. Low-momentum pions intersecting shielding material in the vicinity of the neutron counter were found to be a source of background triggers. These events were also removed from the data and the acceptance programme. After these cuts a total of 18 900 and 15 800 events at 12 and 15 GeV/c, respectively, remained for physics analysis.

The neutron time-of-flight trigger restricted the momentum transferred squared to the neutron, t, to the range -0.02 to -0.8 (GeV/c)^2. The geometrical acceptance of the neutron counter, which subtended angles between 45° and 75° to the beam, imposed further restrictions at low $|t|$ values. Fig. 1 shows the t acceptance at low $|t|$ as a function of the recoil $\pi^+\pi^-\pi^0$ mass at 12 and 15 GeV/c. Also shown are the lines $t = t_{min}$ and $t' = t - t_{min} = 0.05$. From fig. 1 it can be seen that

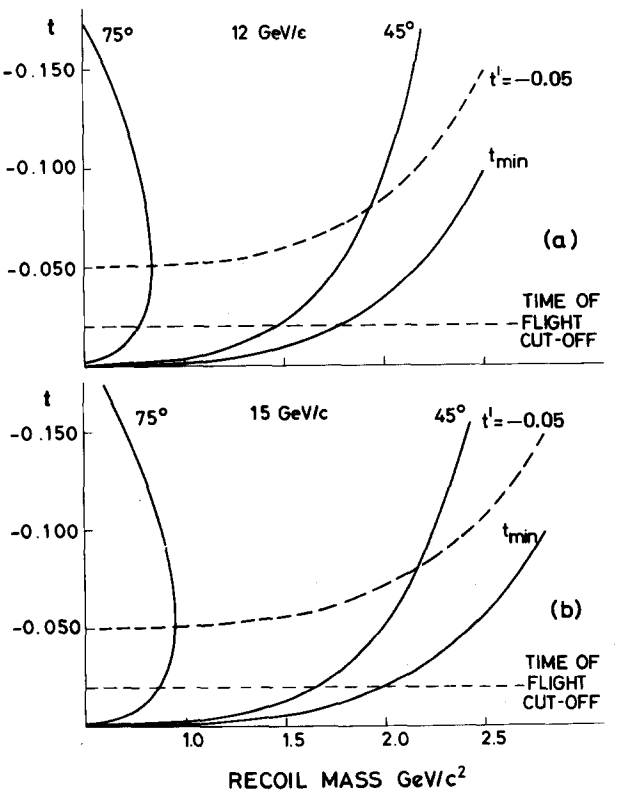

Fig. 1. t acceptance as a function of the recoil $\pi^+\pi^-\pi^0$ mass: (a) at 12 GeV/c, (b) at 15 GeV/c.

removing events with $t' > -0.05$ ensures a slowly varying $\pi^+\pi^-\pi^0$ mass acceptance up to 1.9 and 2.2 GeV/c^2 at 12 and 15 GeV/c respectively. For the partial-wave analysis we have therefore used events in the t' range $-0.6 < t' < -0.05$.

Fig. 2 shows the $\pi^+\pi^-\pi^0$ effective-mass plots for events in the t range $-0.02 > t > -0.8$ and the hatched histograms for events in the t' range $-0.05 > t' > -0.6$. Clear signals for $\eta(548)$, $\omega(780)$, $A_2^0(1310)$ and $\omega^*(1675)$ are observed at both 12 and 15 GeV/c. Results on the $\omega(780)$ [12], $A_2^0(1310)$ and $\omega^*(1675)$ [9] have already been published. In the 15 GeV/c data an enhancement is observed around 2.0 GeV/c^2. At 12 GeV/c this peak is suppressed by the high-mass cut-off of the apparatus, which is 300 MeV/c^2 lower than at 15 GeV/c. Fig. 3 shows the π^0n, π^+n and π^-n effective masses for the 15 GeV/c data. A clear low-mass Δ/N^* peak is seen in π^0n but not in the other combinations. Similar plots are observed at 12 GeV/c.

To remove Δ and N^* isobar events cuts were applied on π^+n and π^0n effective masses squared less than 1.8 and 3.0 $(\text{GeV}/c^2)^2$, respectively, with the additional requirement that the momentum transfer squared to the πn system be less than 0.2 $(\text{GeV}/c)^2$. This latter requirement has been imposed since Δ/N^* production is highly peripheral. The exponential slope of the differential cross section

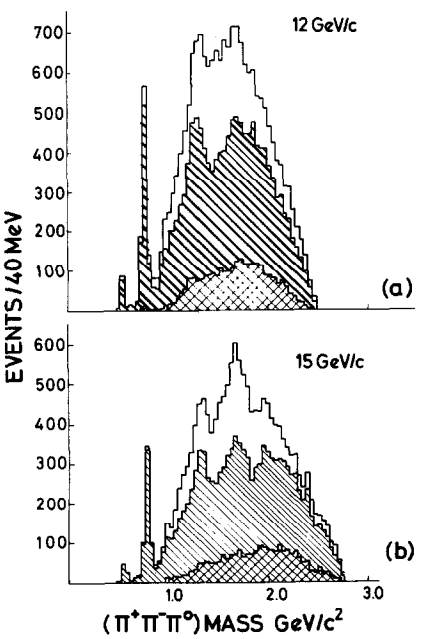

Fig. 2. $\pi^+\pi^-\pi^0$ effective-mass plots: (a) at 12 GeV/c, (b) at 15 GeV/c. Total histogram for events in the t range $-0.02 > t > -0.8$, crossed histogram for events in the t' range $-0.05 > t' > -0.6$ and cross-hatched histogram is Δ/N^* contribution removed for analysis.

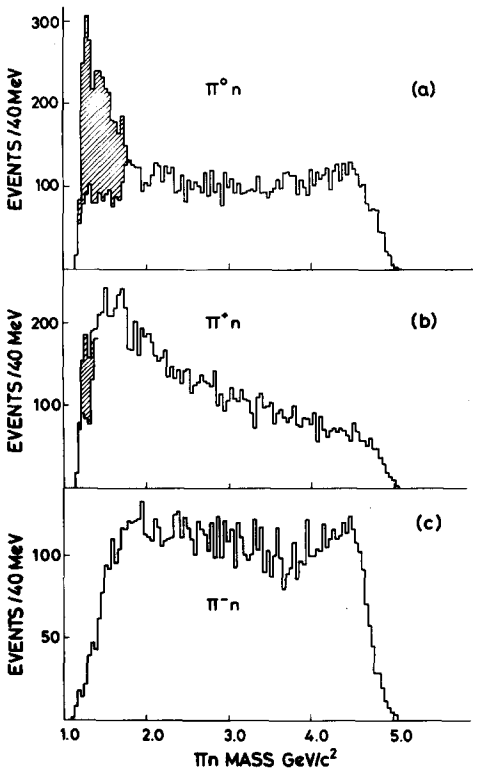

Fig. 3. πn effective-mass plots at 15 GeV/c, (a) π^0n, (b) π^+n, (c) π^-n. Crossed area is Δ/N^* contribution removed for analysis.

(14.5 at 11.7 GeV/c) [13] would imply that 95% of the Δ/N^* production is removed by this cut. The events removed by this cut exhibit strong ρ production similar to that observed by the authors of ref. [13]. The harder cut on the π^0n effective mass is imposed in order to remove any $\rho^0\Delta$ events which in the three-pion partial-wave analysis would result in misfitting the $I = 0$ contribution to $\rho^0\pi^0$. Three-pion $I = 0$ states can contribute to $\rho^\pm$ and ρ^0 production whereas $I = 1$ states can only contribute to $\rho^\pm$ production. The cross-hatched histogram in fig. 2 and the shaded areas in fig. 3 are the contributions within the $-0.6 < t' < -0.05$ cut from Δ and N^* isobars which are subsequently removed in the analysis.

Fig. 4 shows the $\pi^+\pi^-$, $\pi^-\pi^0$ and $\pi^+\pi^0$ effective masses for the 12 and 15 GeV/c data after all cuts have been applied. Strong ρ production is observed in all three charged states.

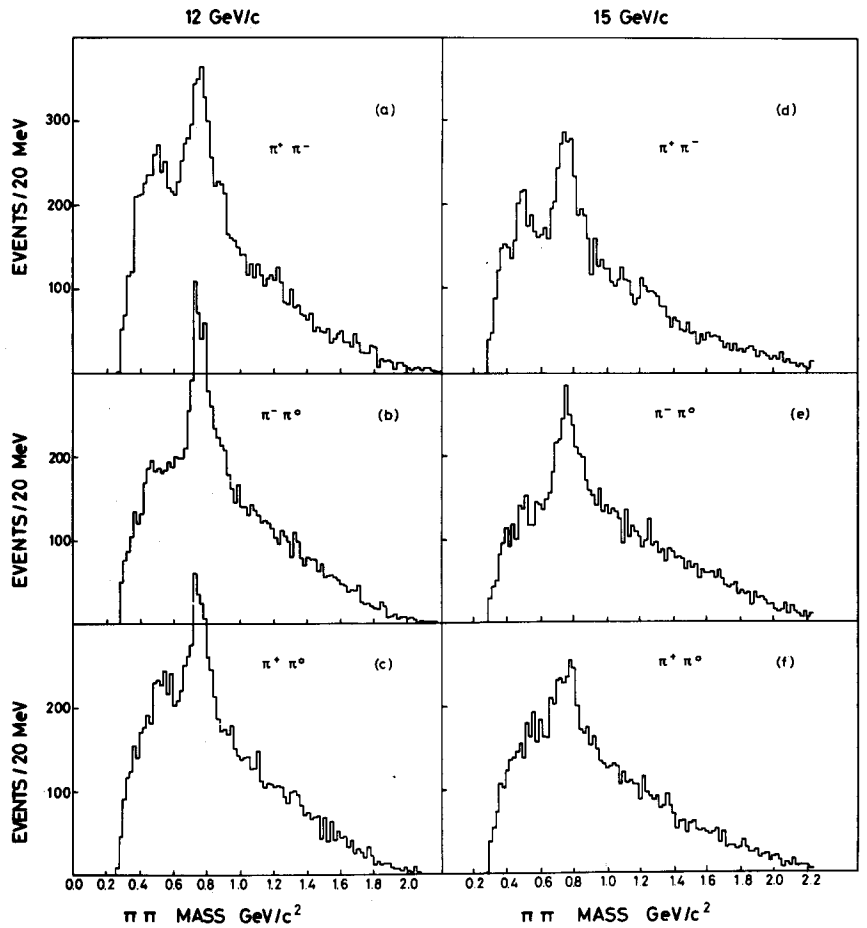

Fig. 4. $\pi\pi$ effective-mass plots after all cuts: (a) $\pi^+\pi^-$, (b) $\pi^-\pi^0$, (c) $\pi^+\pi^0$ at 12 GeV/c; (d) $\pi^+\pi^-$, (e) $\pi^-\pi^0$, (f) $\pi^+\pi^0$ at 15 GeV/c.

3. Method of analysis

We have used a programme based on that developed at the University of Illinois and modified for the charge-exchange reaction $\pi^+ n \to \pi^+\pi^-\pi^0 p$ by Emms et al. [4]. In this type of analysis the states of the 3π system produced are parameterised in terms of the density matrix ρ and the decay of the 3π system in terms of an isobar model. The density matrix is constructed from partial waves each of definite isospin I, spin-parity and spin projection $J^P M$, and the relative orbital angular momentum L of the π and dipion system [7]. The partial waves are thus represented by the eigenstates $|I J^P L M \eta\rangle$, where η corresponds, at high

energies, to the naturality of the exchange mechanism. In this analysis the isobar-π states used were $\epsilon\pi$ and $f^0\pi$, which are pure $I = 1$ states, and $\rho\pi$ and $g\pi$ which can be $I = 0$, 1 or 2. S-wave $\pi^+\pi^-$ phase shifts [14] have been taken to parameterize the ϵ, while relativistic Breit-Wigner forms have been used for the ρ, g and f^0. The analysis was preformed in the t-channel.

The partial-wave programme takes into account the acceptance and inefficiencies of the apparatus and the cuts made on the data. The acceptance normalisation integrals were evaluated by generating Monte Carlo events and tracking them in a simulated apparatus. From angular momentum considerations the shape of the differential cross section was parameterised by the functional form

$$\frac{d\sigma}{dt'} \propto t'^{M} e^{bt'} , \tag{2}$$

where M is the spin projection and b is the slope parameter.

For the unnatural spin-parity states the slope b was determined by maximising the likelihood in 160 MeV/c^2 mass bins. From these fits a good description of the slope as a function of 3π mass $m_{3\pi}$ was found to be

$$b = (4.5 \pm 0.6) + (2.3 \pm 0.3)\, m_{3\pi} \qquad \text{at 12 GeV/}c\,,$$

$$(5.6 \pm 0.3) + (1.8 \pm 0.4)\, m_{3\pi} \qquad \text{at 15 GeV/}c\,.$$

For the natural spin-parity states the slope b was assumed to be a linear function of $\ln(m_{3\pi}^2/s)$. This functional form was inspired by ref. [15] and demonstrated for our data in ref. [9]. A different method was adopted in determining b in this case. The differential cross sections for each resonance ($\omega(780)$, $A_2^0(1310)$ and $\omega^*(1675)$) were obtained by performing fits in small t' intervals. The slope was then obtained for each resonance at 12 and 15 GeV/c by fitting formula (2) to these differential cross sections. Using these slopes gave

$$b = (2.0 \pm 0.5) - (1.74 \pm 0.47) \ln(m_{3\pi}^2/s)\,.$$

These parameterizations for b were then used throughout the analysis.

Extensive searches for the most important partial waves were carried out independently with the 12 and 15 GeV/c data. The number of partial waves tried was limited by only considering waves with the lowest possible L value and $M \leqslant 1$. Solutions obtained at lower masses were used to provide starting values for searches at higher masses. The same set of dominant waves was obtained at both momenta and therefore the data were combined for the subsequent fits. Final searches were then made in 80 MeV/c^2 mass intervals up to a mass of 1.96 GeV/c^2. The total contribution to a given spin-parity and the principal waves were found to be stable against the addition of other waves.

4. Results of the analysis

The following $IJ^PLM\eta$ states were found to be strongly populated:

$10^-S0 + (\epsilon\pi)$, $10^-P0 + (\rho\pi)$,

$01^+S0 + (\rho\pi)$, $11^+P0 + (\epsilon\pi)$,

$11^+S0 + (\rho\pi)$, $12^-P0 + (\rho\pi)$,

$12^-D0 + (\epsilon\pi)$, $12^-S0\,(f\pi)$,

$11^+P1 + (\epsilon\pi)$.

Above a 3π mass of 1.56 GeV/c^2, spin-parity 3^+ appears to be required by the data, the wave $03^+D0 + (\rho\pi)$ giving the highest likelihood. In addition the states $01^-P0 - (\rho\pi)$, $01^-P1 \pm (\rho\pi)$ are necessary in the $\omega(780)$ mass region, $12^+D0 - (\rho\pi)$ in the A_2^0 mass region and $03^-F0 - (\rho\pi)$, $03^-F1 \pm (\rho\pi)$ in the $\omega^*(1675)$ mass region and above. Generally for the unnatural parity states $\rho\pi$ decay modes are more important at low masses and $\epsilon\pi$ decay modes at higher masses. Furthermore, significant $I = 0$ contributions are only observed in the $J^PLM\eta = 1^+S0 +$ and 3^+D0+ states.

4.1. Unnatural spin-parity states

In fig. 5 the intensities of the various unnatural spin-parity contributions are presented. The bands are predictions of a reggeized Deck model calculation to be discussed below. Here, it can be seen that the total $J^PM\eta = 0^-0+$ contribution is almost flat throughout the fitted mass region. The bin 0.92 to 1.00 GeV/c^2 contains some contamination from $\eta' \to \pi\pi\gamma$ events which are kinematically misfitted as $\pi^+\pi^-\pi^0$. This is consistent with the number of $\eta' \to \eta\pi\pi$ events observed in the channel $\pi p \to \pi^+\pi^+\pi^-\pi^-\pi^0 n$ in this experiment. Such η' events have also been observed in the reaction $K^-p \to \Lambda\pi^+\pi^-\pi^0$ at 4.2 GeV/c [6]. The 2^-0+ contribution shows a slow rise with mass with the $\epsilon\pi$ decay mode being largest at higher masses, the $\rho\pi$ being more important at lower masses and the $f^0\pi$ being flat throughout the mass range.

The $J^P = 1^+$ partial wave gives the largest contribution to the $(3\pi)^0$ cross section. For the 1^+0+ contribution there is a rise with mass similar to that of the 2^-0+ contribution, but with an additional structure around 1.1 GeV/c^2.

By splitting the 1^+0+ contribution into its constituents, figs. 5d, e, f, it can be seen that this structure is almost entirely due to the $I = 0$ $\rho\pi$ wave. The $\rho\pi$ component of the $I = 1$ partial waves is almost flat throughout the fitted mass region while the $\epsilon\pi$ component shows a sharp rise in intensity at a $(3\pi)^0$ mass of about 1.3 GeV/c^2. The only $M \neq 0$ unnatural parity state found to be strongly populated is the $11^+P1 + (\epsilon\pi)$ partial wave. This wave, shown in fig. 5g, rises sharply at a

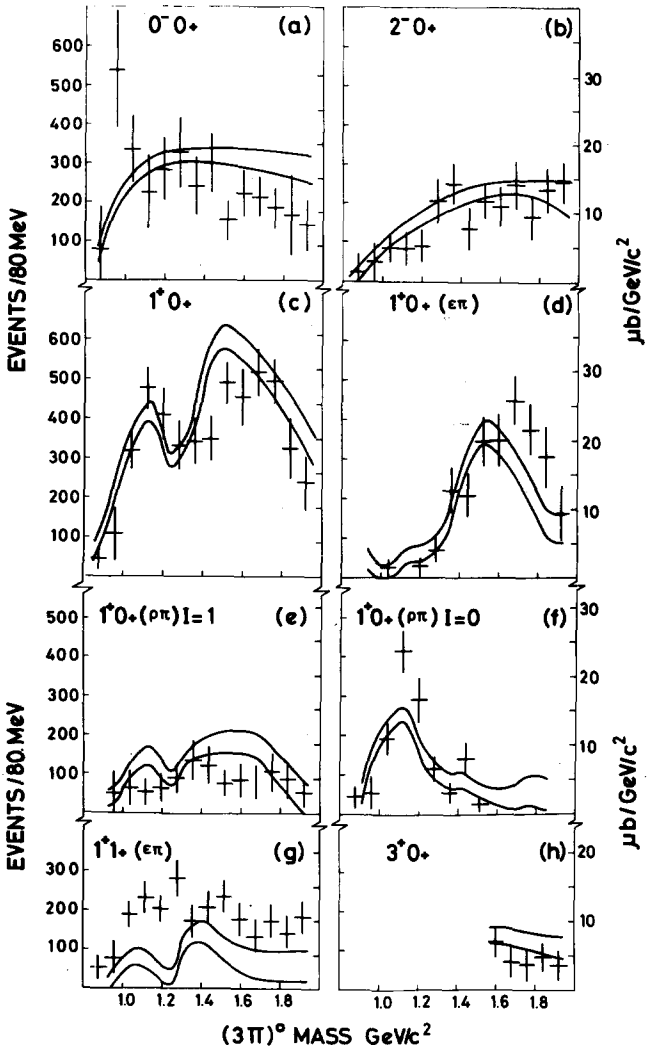

Fig. 5. Intensities of the unnatural spin-parity waves corrected for acceptance as a function of 3π mass:

(a) 0^-0+, (b) 2^-0+,

(c) 1^+0+, (d) $1^+0+(\epsilon\pi)$,

(e) $1^+0+(\rho\pi)$, $I=1$, (f) $1^+0+(\rho\pi)$, $I=0$,

(g) 1^+1+, (h) 3^+0+.

The bands are the predictions of the Deck model calculation (see text).

$(3\pi)^0$ mass of 1.0 GeV/c^2 and then falls slowly with mass.

In fig. 6 the phases of the $J^P = 1^+$ waves are shown relative to other waves, namely $IJ^PLM\eta = 12^-\text{P0}+(\rho\pi)$ and $10^-\text{S0}+(\epsilon\pi)$. These waves exhibited a smooth mass dependence and had coherences with the $J^P = 1^+$ waves consistent with unity. The phases shown were found to be fairly stable between different fits. For a resonance on a small background a relative phase change of approximately 180° would be expected. That such a trend is not observed in the $J^P = 1^+$ waves is consistent with previous three-pion partial-wave analyses.

Removing events at $|t'|$ less than 0.05 (GeV/c)^2 suppresses the unnatural spin-parity states relative to the natural spin-parity states. In order to enhance the unnatural spin-parity states we have therefore also analysed the data in the t' range −0.02 to −0.2 (GeV/c)^2. For full coverage of this t' range the $(3\pi)^0$ mass is restricted by our apparatus to the range 0.9 to 1.6 GeV/c^2. Similar results to those presented above were obtained from the analysis. The structure of the $J^P = 1^+$ waves was the same and the relative phases were flat.

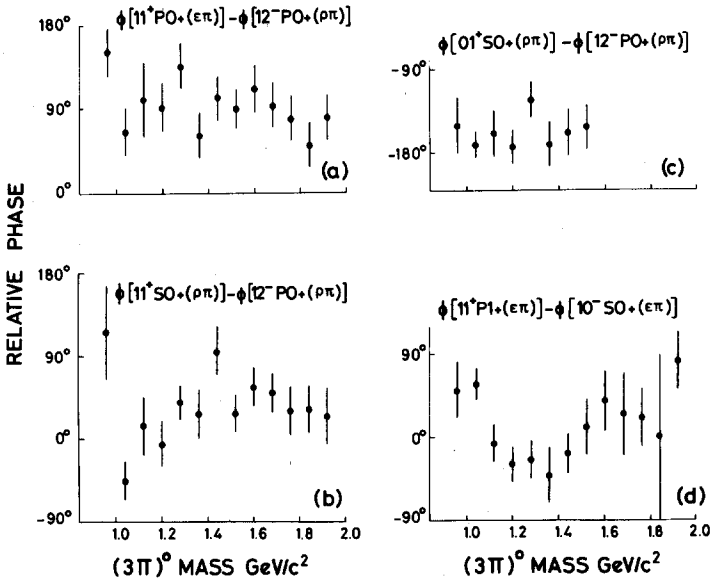

Fig. 6. Relative phases of $J^P = 1^+$ partial waves as a function of 3π mass:

(a) $\phi[11^+\text{P0} + (\epsilon\pi)] - \phi[12^-\text{P0} + (\rho\pi)]$,

(b) $\phi[11^+\text{S0} + (\rho\pi)] - \phi[12^-\text{P0} + (\rho\pi)]$,

(c) $\phi[01^+\text{S0} + (\rho\pi)] - \phi[12^-\text{P0} + (\rho\pi)]$,

(d) $\phi[11^+\text{P1} + (\epsilon\pi)] - \phi[10^-\text{S0} + (\epsilon\pi)]$.

4.2. The high-mass enhancement and natural spin-parity states

The intensities of the various natural parity states are shown in fig. 7. It can be seen that the $IJ^P = 01^-$, 12^+ and 03^- partial waves exhibit enhancements which are assumed to be the $\omega(780)$, $A_2^0(1310)$ and the $\omega^*(1675)$ resonances. The production of these resonances is discussed elsewhere [9,12].

In the region of the high-mass enhancement at 2 GeV/c^2 observed in the 15 GeV/c data, partial waves up to and including spin-4 have been tried. Individual partial waves have been added to a basic set and the relative log likelihoods obtained from the fits compared. The basic set contained the unnatural parity waves

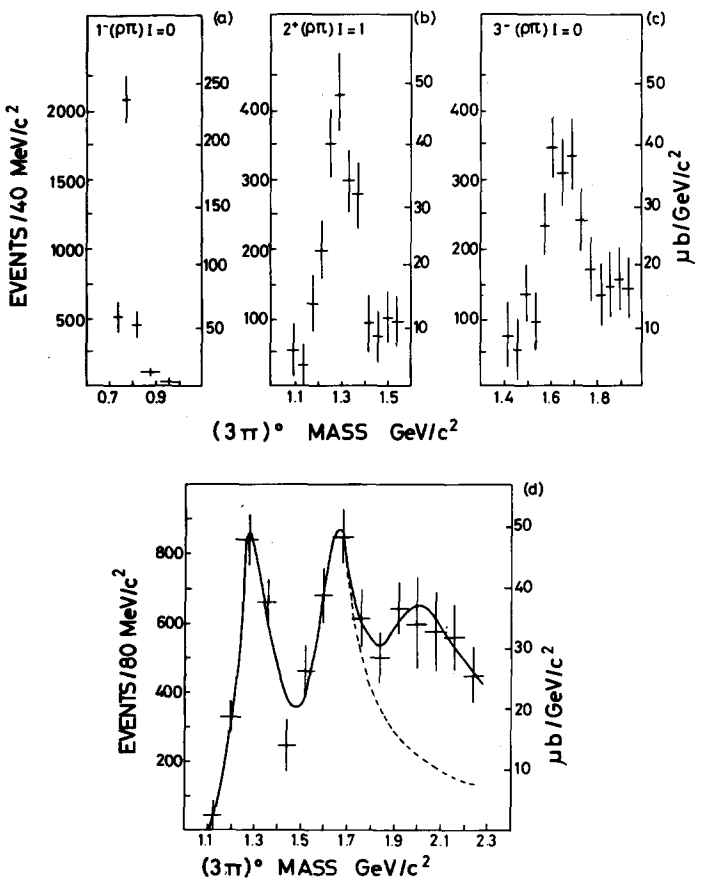

Fig. 7. Intensities of the natural spin-parity waves corrected for acceptance as a function of 3π mass: (a) total $J^P = 1^-$, $I = 0$ contribution, (b) total $J^P = 2^+$, $I = 1$ contribution, (c) total $J^P = 3^-$, $I = 0$ contribution, (d) combined natural spin-parity contribution above 1 GeV/c^2.

listed above and the 03^- waves. For the 3π mass bin 1.92 to 2.16 GeV/c^2 table 1 gives the 15 highest log likelihoods obtained and the extra wave added in each case. We consider a change in the log likelihood of about 20 to be significant. Inspection shows that an $I = 1$ natural parity wave is favoured, with $J^P = 4^+$ slightly preferred over $J^P = 2^+$. Including a $J^P = 4^+$ wave with both $\rho\pi$ and $g\pi$ decay modes together resulted in a dominant $\rho\pi$ mode and strong destructive interference between (ρ^+, g^-) and between (ρ^-, g^+). The total contribution to $J^P = 4^+$ with and without the $g\pi$ mode was found to be the same. Because of these observations, together with the lack of any g signal in the $\pi\pi$ effective mass plots (fig. 4), we have fitted the $J^P = 4^+$ contribution with the $\rho\pi$ decay mode only.

When the fits were repeated in narrower (80 MeV/c^2) mass bins above 1.72 GeV/c^2 it was not possible to distinguish between fits including $J^PL = 4^+G$ or 2^+D partial waves. Furthermore strong correlations were observed between these additional waves and the $J^PL = 3^-F$ waves. A similar but smaller effect was noted in the overlap region of the A_2^0 and $\omega^*(1675)$. No strong correlations were observed between the natural and unnatural parity waves. However the total natural spin-parity contribution was found to be stable between different fits and a typical fit is shown in fig. 7d. In this plot an enhancement in the 2 GeV/c^2 mass region can be seen which may be interpreted as a broad $IJ^P = 14^+$ or 12^+ resonance lying on the tail of the $\omega^*(1675)$. The solid curve on the plot is the prediction from a fit to the data of a sum of three Breit-Wigners and the dashed curve the predicted contribution from the $A_2^0(1310)$ and $\omega^*(1675)$ only. Relativistic Breit-Wigner

Table 1
The top 15 fits obtained in the $(3\pi)^0$ mass bin 1.92 to 2.16 GeV/c^2 for the hypotheses of a basic set of waves (see text) with an additional wave

	Additional wave $IJ^PLM\eta$	Log likelihood
1	$14^+D1 - (g\pi)$	−1961
2	$14^+G1 + (\rho\pi)$	−1965
3	$14^+D0 - (g\pi)$	−1971
4	$12^+D1 + (\rho\pi)$	−1979
5	$14^+D1 + (g\pi)$	−1996
6	$14^-P0 + (g\pi)$	−1997
7	$04^+G1 + (\rho\pi)$	−2001
8	$01^-P1 + (\rho\pi)$	−2016
9	$12^+P1 + (f\pi)$	−2019
10	$14^+F1 + (f\pi)$	−2020
11	$14^+G1 - (\rho\pi)$	−2032
12	$04^+D1 + (g\pi)$	−2034
13	$04^-P0 + (g\pi)$	−2035
14	$13^+S0 + (g\pi)$	−2039
15	$03^+S0 + (g\pi)$	−2048

forms were used which have the following parametrisation:

$$\mathrm{BW}(m) = \frac{m}{q}\,\frac{(m_0\Gamma)^2}{(m^2 - m_0^2)^2 + (m\Gamma)^2}\,, \tag{3}$$

$$\Gamma = \Gamma_0\left(\frac{q}{q_0}\right)^{2L+1}\frac{D_L(q_0 r)}{D_L(qr)}\,,$$

where m_0, Γ_0 and q_0 are the mass, width and c.m. decay momenta at resonance, D_L are Blatt and Weisskopf barrier penetration factors and r is the range parameter set to 1 fm.

L values of 2, 3 and 4 were used for the $A_2^0(1310)$, $\omega^*(1675)$ and the high-mass enhancement respectively. The parameters found for the enhancement were m_0 = (2.03 ± 0.05) and Γ_0 = (0.51 ± 0.20). Using an L value of 2 did not significantly change these values. We propose to call this effect the $A_2^*(2030)$.

The natural spin-parity states were found to be incoherent with the unnatural spin-parity states. It was therefore not possible to extract sensible phase information. This incoherence indicates a different production mechanism for the unnatural and natural spin-parity states. Further evidence for a different mechanism comes from the mass dependence of the slope parameter b. For natural (unnatural) spin-parity states b decreases (increases) as the three-pion mass increases.

5. Comparison of the fits with the data

Checks have been made to ascertain whether the fits reliably reproduce all features of the data. Monte Carlo events have been generated according to the solutions obtained from the fits. The resulting 1-dimensional plots of these Monte Carlo events compare well with the data. However the fits fail to reproduce the peaking in the $n\pi^+$ effective mass below 1.8 GeV/c^2, indicating a small residual N^{*+} contamination of approximately 4%. Increasing the $n\pi^+$ effective mass squared cut from 1.8 to 3.0 (GeV/c^2)^2 gave results similar to those described above and so this cut was kept at its lower value.

Fig. 8 shows the dipion effective-mass plots and predictions for events selected to represent the A_2^0 and $\omega^*(1675)$ regions, namely 1.24 to 1.40 and 1.56 to 1.88 GeV/c^2 respectively. Strong production of $\rho^\pm$ is observed in both regions and of ρ^0 in the $\omega^*(1675)$ region. This clearly demonstrates the dominance of $I = 1$ states in the A_2^0 region and the presence of a strong $I = 0$ signal in the $\omega^*(1675)$ region. At the higher $(3\pi)^0$ effective masses small discrepancies occur above about 1 GeV/c^2 in the $\pi^+\pi^-$ effective mass. These discrepancies are due to our phase-shift parameterisation of the s-wave $\pi^+\pi^-$ system. The intensity of the s-wave $\pi^+\pi^-$ system is predicted to have a dip at about 1 GeV/c^2 due to the onset of the $K\bar{K}$ threshold and then peaks again just above 1.2 GeV/c^2. The structure in the Monte Carlo prediction at 1.2 GeV/c^2 (solid line in fig. 8f) does not come

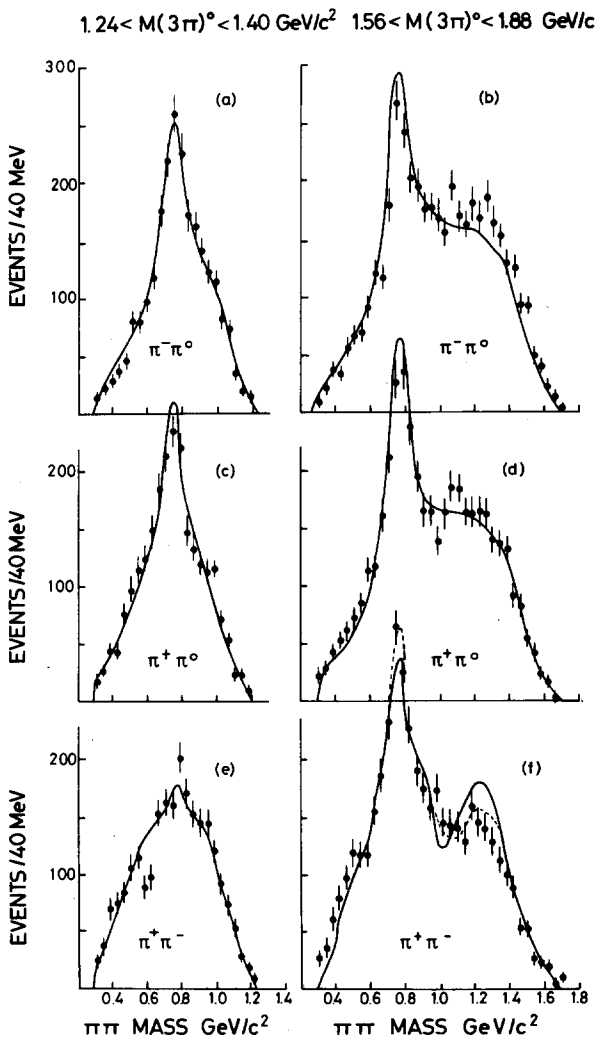

Fig. 8. Monte Carlo predictions (line) compared with the raw data (points) for events in the 3π mass ranges 1.24 to 1.40 GeV/c^2 (a, c, e) and 1.56 to 1.88 GeV/c^2. (b, d, f). (a, b) $\pi^-\pi^0$ effective masses, (c, d) $\pi^+\pi^0$ effective masses, (e, f) $\pi^+\pi^-$ effective mass. For explanation of dashed curve on fig. 8f see text.

from f^0 production since the fitted f^0 contribution is too small. Slightly better fits were obtained to our data at higher $(3\pi)^0$ effective masses using a Breit-Wigner parameterisation of the ϵ, the mass and width being fixed at 0.75 and 0.4 GeV/c^2, respectively. The dashed curve in fig. 8f is the prediction using the ϵ Breit-Wigner

parameterisation. The fitted parameters exhibit no marked differences from previous fits.

Fig. 9 shows the Euler angles ϕ, $\cos\theta$ and γ with the Monte Carlo predictions from the fit for the A_2^0 and $\omega^*(1675)$ mass regions 1.24 to 1.40 GeV/c^2 and 1.56 to 1.88 GeV/c^2, respectively. Both data and fit shown in figs. 8 and 9 are uncorrected for acceptance and the $n\pi^+$ effective mass squared cut is at the higher value

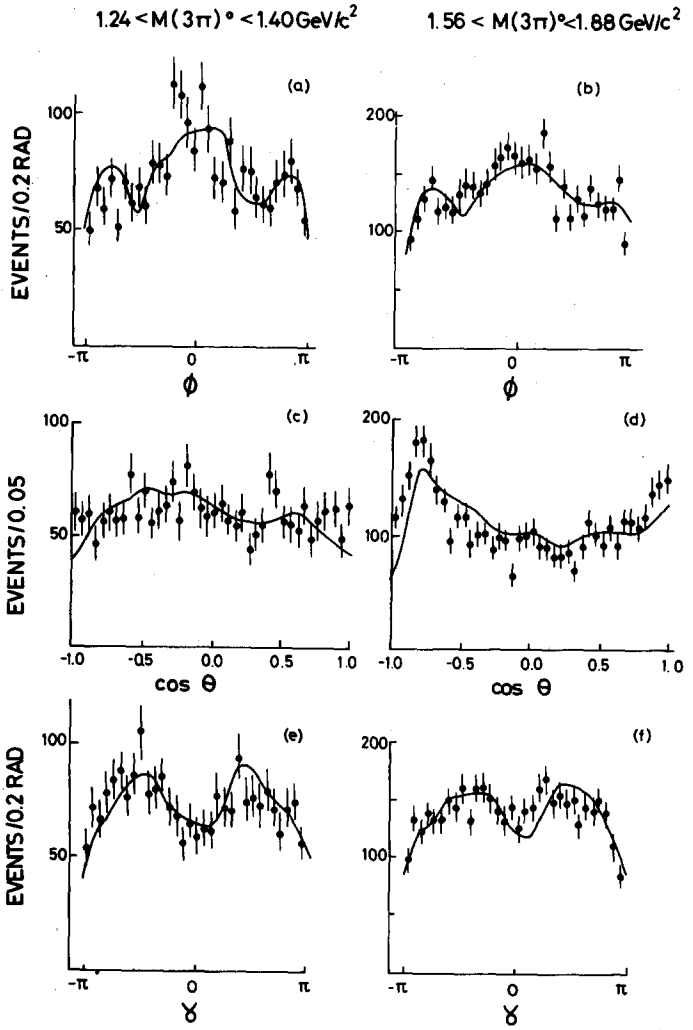

Fig. 9. Monte Carlo predictions (line) compared with the raw data (points) for events in the 3π mass ranges 1.24 to 1.40 GeV/c^2 (a, c, e) and 1.56 to 1.88 GeV/c^2 (b, d, f). (a, b) ϕ, (c, d) $\cos\theta$, (e, f) γ. In this analysis the π^0 has been used as the analyser.

of 3.0 $(\mathrm{GeV}/c^2)^2$ as discussed above. These cuts tend to distort the angular distributions and so make their interpretation complicated.

6. Comparison with a Deck model

We have used the Monte Carlo programme of Ascoli et al. [2] suitably modified for our reaction in order to predict the absolute cross sections for the Deck process at 12 and 15 GeV/c beam momenta. The model utilizes the experimental $\pi\pi$ phase shifts and πN amplitudes, and combines them with a reggeized pion propagator (fig. 10). Events were generated with 3π effective mass in the region $0.92 \leqslant m_{3\pi} \leqslant 1.96$ GeV/c^2. A total of 2000 events per 40 MeV/c^2, at each beam energy, were generated and subsequently analysed in exactly the same way as the data. In fig. 5 the bands are the predictions of the reggeized Deck model for the contributions of the unnatural-parity waves. These are absolute predictions and are not fits to the data. They may not necessarily represent a complete partial-wave decomposition since only the waves found in the data were used. The predictions for the natural-parity states were finite but never more than 15 events per 40 MeV/c^2 effective-mass bin.

It can be seen that the predictions are in reasonable agreement with the data. The $J^PM\eta = 0^-0+$ contribution is featureless throughout the fitted mass region and the 2^-0+ contribution rises slowly with mass. The structure in the 1^+0+ contribution is due to threshold enhancements in the $\rho\pi$ and $\epsilon\pi$ decay modes. The peak at 1.1 GeV/c^2 in the $\rho\pi$ $I = 0$ component and the sharp rise at 1.4 GeV/c^2 in the $\epsilon\pi$ $I = 1$ contribution are both predicted by the model. The $\rho\pi$ $I = 1$ component of the 1^+ wave is in only qualitative agreement in fig. 5e: however there is no evidence for an A_1 meson. In fig. 5g there is an excess of events in the $1^+1+(\epsilon\pi)$ partial wave above the prediction in the effective-mass region 1.0 to 1.3 GeV/c^2. Whether this excess is due to a 1^+ resonance or just reflects the inadequacy of this model in predicting the $M = 1$ partial waves is impossible to determine from our data.

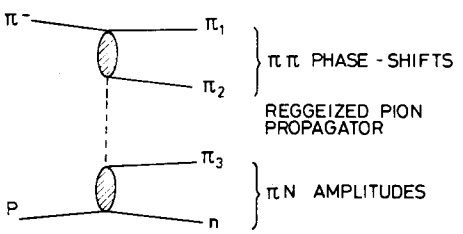

Fig. 10. Schematic representation of the Deck model used to describe the unnatural spin-parity waves as shown in fig. 5.

7. Conclusions

A partial-wave analysis of the $\pi^+\pi^-\pi^0$ system produced in the reaction $\pi^-p \to \pi^+\pi^-\pi^0 n$ at 12 and 15 GeV/c has been performed. Strong production of the natural spin-parity resonances $\omega(780)$, $A_2^0(1310)$ and $\omega^*(1675)$ is observed. In addition, a broad mass enhancement, the $A_2^*(2030)$, with a mass (2.03 ± 0.05) GeV/c^2 and width (0.51 ± 0.20) GeV/c^2 is observed. Spin-parity 4^+ is favoured, though 2^+ cannot be excluded. A clear separation of this additional wave is not possible because of the strong overlap with the tail of the $\omega^*(1675)$. A Regge trajectory through the $A_2^0(1310)$, degenerate with the $\omega(780)$, $\omega^*(1675)$ trajectory, would predict a spin-4 resonant state at a mass of ~1.97 GeV/c^2.

There is no evidence for an A_1 resonance decaying to $\rho\pi$ or an A_3 decaying to $f^0\pi$. An upper limit on the ratio of the A_1 to A_2^0 production cross sections can be obtained by assuming that all the $1^+0+(\rho\pi)$ contribution below 1.3 GeV is due to A_1 production. This amounts to ~4μb/GeV and the similar figure for the peak of the A_2^0 production is 48 μb/GeV. Hence the A_1 peak production cross section is at least an order of magnitude smaller than that for A_2^0 production. However the reggeized Deck model prediction for the $1^+0+(\rho\pi)$ wave implies a considerably smaller production cross section for the A_1. Two $I = 0, J^{PC} = 1^{+-}$ resonances are required by the constituent quark model. A sharp $I = 0$ enhancement is observed at 1.14 GeV/c^2 in the $J^P = 1^+$ wave over and above the reggeized Deck model calculation though the measured phase variation is flat. Generally the unnatural spin-parity states are well described in terms of a reggeized Deck model [2].

The natural spin-parity states were found to be incoherent with the unnatural spin-parity states. The natural and unnatural spin-parity states were found to have different mass dependences of the slope parameter for the differential cross section. These two observations suggest different production mechanisms for the natural and unnatural spin-parity states. From refs. [12,9] the production of the ω^0 and A_2^0 respectively are shown to be described in terms of a simple Regge model exchanging ρ- and B-like trajectories. However the semi-quantitative agreement of the reggeized Deck model calculation suggests a Deck type of production mechanism for the unnatural spin-parity states.

We are most indebted to the Omega Group at CERN for their efficiency and expertise in providing and maintaining the facilities of the spectrometer. We would like to thank Drs. D.J. Crennell, J.D. Hansen, K. Paler and S.N. Tovey for useful discussions on the analysis programmes.

References

[1] G.W. Brandenburg et al., Phys. Rev. Lett. 36 (1976) 703;
G.W. Brandenburg et al., Phys. Rev. Lett. 36 (1976) 706.

[2] G. Ascoli et al., Phys. Rev. D8 (1973) 3894;
G. Ascoli et al., Phys. Rev. D9 (1974) 1963.
[3] R.J. Hemingway, Raporteur's talk at European Conf. on particle physics, Budapest, July 1977, CERN/EP/PHYS 77–41.
[4] M.J. Emms et al., Phys. Lett. 58B (1975) 117.
[5] F. Wagner et al., Phys. Rev. Lett. 58B (1975) 201.
[6] M. Cerrada et al., Nucl. Phys. B126 (1977) 241.
[7] J.D. Hansen et al., Nucl. Phys. B81 (1974) 403.
[8] J. Garvey, Int. Conf. on instrumentation for high-energy physics, Frascati, 1973;
M.J. Corden et al., Rutherford Lab. preprint RL77 074/A.
[9] M.J. Corden et al., Rutherford Lab. preprint RL77 097/A.
[10] F. Bourgeois, H. Grote and J.-C. Lassalle, Pattern recognition methods for Omega and SFM spark chamber experiments, CERN/DD/DH/70-1;
H. Grote, M. Hansroul, J.-C. Lassalle and P. Zanella, Identification of digitised particle trajectories, International computing symp., 1973 (North-Holland, Amsterdam, 1974).
[11] Rutherford Laboratory kinematical fitting programme NIRL/M/38.
[12] J.D. Dowell et al., Nucl. Phys. B108 (1976) 30.
[13] R.O. Maddock et al., Nuovo Cim. 5A (1971) 457.
[14] B. Hyams et al., Nucl. Phys. B64 (1973) 134.
[15] P. Hoyer, R.G. Roberts and D.P. Roy, Nucl. Phys. B56 (1973) 173.